"Crocidolite Dissolution in the Presence of Fe Chelators: Implications for Mineral-Induced Disease"

by

Andrew J. Werner

Thesis submitted to the Faculty of
Virginia Polytechnic Institute and State University
in partial fulfillment of the requirements of the degree of

MASTER OF SCIENCE
in
GEOLOGY

APPROVED:

Michael F. Hochella, Jr.
Chairman

George D. Guthrie, Jr.

J. Donald Rimstidt

July, 1994

Blacksburg, Virginia

Crocidolite Dissolution in the Presence of Fe Chelators: Implications for Mineral-Induced Disease

by

Andrew J. Werner

Committee Chairman: Michael F. Hochella, Jr.
Geological Sciences

(ABSTRACT)

Some asbestiform minerals may cause lung disease in humans such as asbestosis, mesothelioma, and lung cancer. Crocidolite, the asbestiform counterpart of the amphibole riebeckite, is particularly dangerous in cases of chronic exposure. Its pathogenic activity may result from the interaction of the fiber surfaces with physiological fluids. Fe removed from the fiber surface by molecular chelators present in the body can promote a series of reactions that yield the hydroxyl radicals ($^{\bullet}OH$) which are known to cause DNA damage. This breakdown of DNA may be part of the mechanism for crocidolite-induced pathogenesis.

X-ray photoelectron spectroscopy (XPS) and solution chemistry were used to monitor the changes in surface composition of crocidolite fibers in a 50 mM NaCl solution at pH=7.5 and 25°C in the presence of Fe chelators (citrate, EDTA, or desferrioxamine) for up to 30 days. The data show that the introduction of Fe chelators dramatically increases the rate at which Fe is released from the surface when compared to a control group where no chelators were added. In particular, XPS shows that Fe(III) is more effectively removed in the presence of the chelators.

Past studies of the dissolution of Fe-containing silicates generally indicate that Fe removal is the rate-limiting step. Fe(III) is particularly insoluble under circumneutral

conditions. However, our work suggests that crocidolite undergoes enhanced dissolution in the presence of a chelator. Therefore, based on our XPS and solution data, and assuming a typical fiber diameter, we can estimate that a crocidolite fiber will survive on the order of hundreds of years in lung-like conditions. This is at least two orders of magnitude longer than a chrysotile fiber of the same size, and corresponds well with the fiber content observed in human lung tissue.

ACKNOWLEDGEMENTS

I would like to thank the members of my committee, Michael F. Hochella, Jr., George D. Guthrie, Jr., and J. Donald Rimstidt for their excellent guidance and their innumerable hours of support throughout this project. Many thanks to Ann E. Aust and Jeanne A. Hardy of Utah State University for their help in gathering the solution chemistry data and their insight into the discipline of biochemistry. Thanks also to Jodi Junta for her never ending patience and infinite sources of information, Cam Weaver and Udo Becker for their many helpful suggestions, and Kevin Rosso for excellent computer support. This research was accomplished through funding from NSF and Los Alamos National Laboratory.

TABLE OF CONTENTS

List of Figures

List of Tables

INTRODUCTION

Asbestiform minerals have been used widely in various industrial and non-industrial applications because of their fibrous shape, high tensile strength, flexibility, long term durability, and fire resistant nature. Currently, the asbestos minerals that are in most common use are the 1:1 sheet silicate chrysotile ($Mg_3Si_2O_5(OH)_4$) and the amphibole crocidolite ($Na_2Fe^{3+}{}_2(Fe^{2+},Mg^{2+})_3Si_8O_{22}(OH)_2$). It is now known that asbestos minerals have the ability to trigger lung-disease in humans such as asbestosis (scarring of lung tissue resulting in lost of lung flexibility), mesothelioma (a malignant tumor of the mesothelial cells which line the lung cavity), and lung cancer, although exactly which mineral is responsible for inducing a particular disease is often debatable (e.g., Wagner et al., 1960; Craighead et al., 1982; Wagner, 1991, Guthrie and Mossman, 1993). Unfortunately, the processes by which certain fibrous minerals induce disease are not known, although a number of important studies have investigated this problem. Stanton et al. (1981) reported a positive correlation between the aspect ratio (length to width) of the fiber and its ability to induce cancer (the Stanton hypothesis); they concluded from tests in rats that fibers with higher aspect ratios are more pathogenic (disease generating). Probably more than any other scientific finding, the Stanton hypothesis has helped shape the current restrictive regulations and guidelines in asbestos use and exposure in the United States (Vu, 1993). In a recent paper, Nolan and Langer (1993) review what is recognized now as major limitations in the Stanton hypothesis; they state that, although the fiber dimension vs. pathogenicity relationship may hold true in some instances, the overall findings of Stanton et al. (1981) are inconclusive insofar as its relevance to human disease. Besides dimension, there are several other aspects of

fibers that can potentially control their deleterious affects on our respiratory systems. For example, fiber durability (i.e., the lifetime of a fiber based on dissolution rate) in lung tissue appears to play an important role (McDonald and McDonald, 1986a,b). Surface characteristics of asbestos fibers, such as charge, composition, structure, and microtopography, may also be influential in dictating how fibers react in and perturb respiratory systems (Hochella, 1993). Even the mechanical properties (stiffness, fragmenting characteristics, etc.) may be important as fibers physically penetrate cell membranes and potentially interfere with cell division (Barrett et al., 1989).

A major implication of most of the studies mentioned above is that there is an important need for an understanding of how minerals respond to physiological fluids. This is likely to be a necessary component of any integrated model of mineral-induced pathogenesis. In this particular study, we have investigated the surface chemistry of iron on crocidolite fibers which have been exposed to fluids that partially mimic lung fluids. We specifically have chosen crocidolite for our work because it is now clear from epidemiological studies (the study of disease in human populations) that it is far more pathogenic than chrysotile. Crocidolite has been shown to promote the occurrence of mesothelioma (e.g., McDonald and McDonald, 1986a) as well as carcinoma (cancer) of the lung and asbestosis (e.g., McDonald and McDonald, 1986b; McDonald, 1990). Furthermore, the surface chemistry of iron on these fibers is of special interest to us because of previous work by Goodglick and Kane (1986), Lund and Aust (1989), and Aust and Lund (1990). These authors suggest that hydroxyl radicals, created by reactions involving iron leached from amphibole asbestos minerals, may be important in mineral-induced disease. In particular, Aust and coworkers studied the release of Fe from crocidolite in the presence of chelators and reducing agents, some of which are present in a physiological fluid (Aust and Lund, 1990, 1991; Lund and Aust, 1992). They reported a link between Fe released from crocidolite and DNA single strand breaks (SSB's) *in*

vitro. Measurement of DNA SSB's is one way of assessing how an agent interacts with DNA, which may be an important component of the disease process. The mechanism used to explain how Fe can cause DNA SSB's is the Haber-Weiss series:

$$\text{Reductant}^{(n)} + \text{Fe(III)} \rightarrow \text{Reductant}^{(n+1)} + \text{Fe(II)} \quad (1)$$

$$\text{Fe(II)} + O_2 \rightarrow \text{Fe(III)} + {}^{\bullet}O_2^{-} \quad (2)$$

$$2\,{}^{\bullet}O_2^{-} + 2H^{+} \rightarrow O_2 + H_2O_2 \quad (3)$$

$$\text{Fe(II)} + H_2O_2 \rightarrow \text{Fe(III)} + OH^{-} + {}^{\bullet}OH \quad (4)$$

In this series of reactions, an Fe atom can be repeatedly cycled between its two valence states, producing highly reactive OH radicals which are detrimental to DNA molecules. By monitoring fluid chemistry, Lund and Aust (1992) showed that when crocidolite is treated with an Fe chelator, Fe is removed from the surface more readily than when the chelator is not present. Furthermore, in solutions of DNA plus crocidolite, SSB's occur at a much higher frequency in the presence of a chelator. These findings suggest that the Fe removed from the surface may be an important factor in mineral-induced disease. Although the post-treatment solutions were analyzed for Fe content in these studies, the mineral surface was not investigated to determine the changes that took place during the reaction with the chelator solution.

Therefore, this study has been specifically designed to begin to unravel the surface chemistry of crocidolite, especially that dealing with both ferrous and ferric iron, as it dissolves under conditions similar to that of a human lung. We have used scanning electron microscopy (SEM) and atomic force microscopy (AFM) to study the fiber shape and surface morphology, as well as X-ray photoelectron spectroscopy (XPS) and solution analysis to track the changes in surface chemistry and the contacting solutions over a 30 day period. In addition, three well-known Fe chelators were chosen for this study, including ethylenediaminetraacetic acid (EDTA), desferrioxamine and citrate. Although citrate is the only one of the three found in the body, EDTA and desferrioxamine were

used as well because they are very effective Fe chelators and both may have application in fiber–surface modification relevant to reducing toxicity of fibers (Brown et al., 1990, Klockars et al., 1990). Ultimately, the results of this study combined with previous work may help lead to a model for mineral-induced pathogenesis that directly includes reactions at the mineral-fluid interface.

MATERIALS AND METHODS

Samples and Reagents

Crocidolite samples were obtained from Dr. Richard Griesemer (National Institute of Environmental Health Sciences/National Toxicology Program, Research Triangle Park, NC). Campbell et al. (1980) report median fiber size of roughly 15.0 x 0.25 μm. The bulk composition was determined by wet chemical methods (Cambell, 1980) and is as follows (in atomic percent): Si 18.6%, Fe(II) 5.9%, Fe(III) 5.4%, Mg 2.1% and Na 3.3%.

Two of the Fe chelators (sodium citrate and disodium salt of EDTA) were obtained from Mallinckrodt, Inc. (Paris, KY). Deferoxamine mesylate USP (desferrioxamine B) was obtained from CIBA (Summit, NJ).

Sample Treatment

Crocidolite (1 mg/mL) was reacted in a 50 mM NaCl solution in glass vials, in air at a pH of 7.5 and room temperature. The pH was initially adjusted to 7.5 using NaOH. The volume of the solution was approximately 50 mL. The solutions were reacted for time periods of 1 hr, 24 hrs, and 30 days in 1 mM citrate, EDTA or desferrioxamine-B. All runs were done in triplicate. One control group was run for each time period without a chelator added. The 30 day runs were resuspended in fresh chelator solutions on the

first and seventh day and the pH was readjusted to 7.5. Each sample was placed on a wrist-action shaker for the first hour and each was kept in the dark to avoid photochemical reduction of ferric iron by the chelators (Chao and Aust, 1992). After the reaction period, the suspension was transferred to 50 mL conical bottom tubes and centrifuged to separate the fibers from the supernatant. Total iron mobilized into the supernatant was measured by the ferrozine method as described in Lund and Aust (1990) except in the case of desferrioxamine where the absorbance of the supernatant was measured directly at 428 nm. The fibers were washed five times in de-ionized water to remove any remaining chelator solution, dried on an acid-washed watch glass at room conditions, and stored in glass vials with screw tops.

Atomic force and scanning electron microscopy

The untreated fibers were examined with a Nanoscope III AFM in air using a silicon nitride tip in constant force mode. Fiber bundles were laid down on double-stick tape, and the tip was repeatedly advanced onto a small group of fibers until images could be obtained on a single fiber without interference from the surrounding sample.

The untreated fibers and the 30 day EDTA, desferrioxamine–B, and citrate–treated fibers were examined with a Noran-Tracor Adem SEM equipped with a LaB6 electron gun. Samples were dispersion mounted on carbon rounds and coated with a 100Å layer of gold.

X-ray photoelectron spectroscopy

Near-surface composition and Fe oxidation state on the crocidolite samples were determined before and after treatment with a Perkin Elmer 5400 XPS (see Hochella, 1988, for a detailed description of XPS). Each sample of crocidolite, in a mat-like form, was mounted on a one inch diameter aluminum stub for examination. A colloidal carbon

suspension (in isopropyl alcohol) was used as a mounting cement. Non-monochromatic Al Kα X-rays (1486.6 eV) were used to analyze a 1 x 3 mm area on the mat of fibers. The Si(2p), Na(2s), Mg(2s), Fe(3p) and C(1s) photolines were used for all analyses. These particular Si, Na, Mg, and Fe photolines were chosen because of their similar binding energies (and thus similar kinetic energies between 1370 and 1440 eV for Al Kα X-rays). Using peaks with similar kinetic energies is important because the electrons that make up these peaks originate from a similar depth in the sample. The C(1s) peak (kinetic energy ≈ 1176 eV) is the only core-level C peak that is attainable for analysis by XPS. The sources of carbon on the surface were the mounting cement and contamination from exposure to the solution and air.

A curve-fitting program (Labcalc) was used to determine the absolute area of the Na(2s) and Fe(3p) peaks (which have a slight overlap) and the Fe(II):Fe(III) ratio (Fig. 1). The Fe(3p) line can be fit best using three peaks, one representing Fe(II) and two representing Fe(III) following the often-cited example of McIntyre and Zeturak (1977). The smaller of the two Fe(III) peaks is needed to account for the numerous multiplet-split peaks that appear on the high binding energy side of the Fe(3p) peak (Gupta and Sen, 1974). The area ratio of the Fe(II) fitted line relative to the two Fe(III) fitted lines is directly proportional to the Fe(II):Fe(III) ratio (Fig. 1).

The Fe(II), Fe(III), Na, Mg, and Si photolines were converted into semi-quantitative compositional data using the following method. The number of atoms present in a given volume is related to the area under a photoline by the equation:

$$I \propto n\sigma \tag{5}$$

where I is the area under the peak, n is the atomic percentage in the measured volume of the sample, and σ is the photoionization cross-section for the sampled orbital for the excitation energy used. The value of σ for each photoline was determined from the

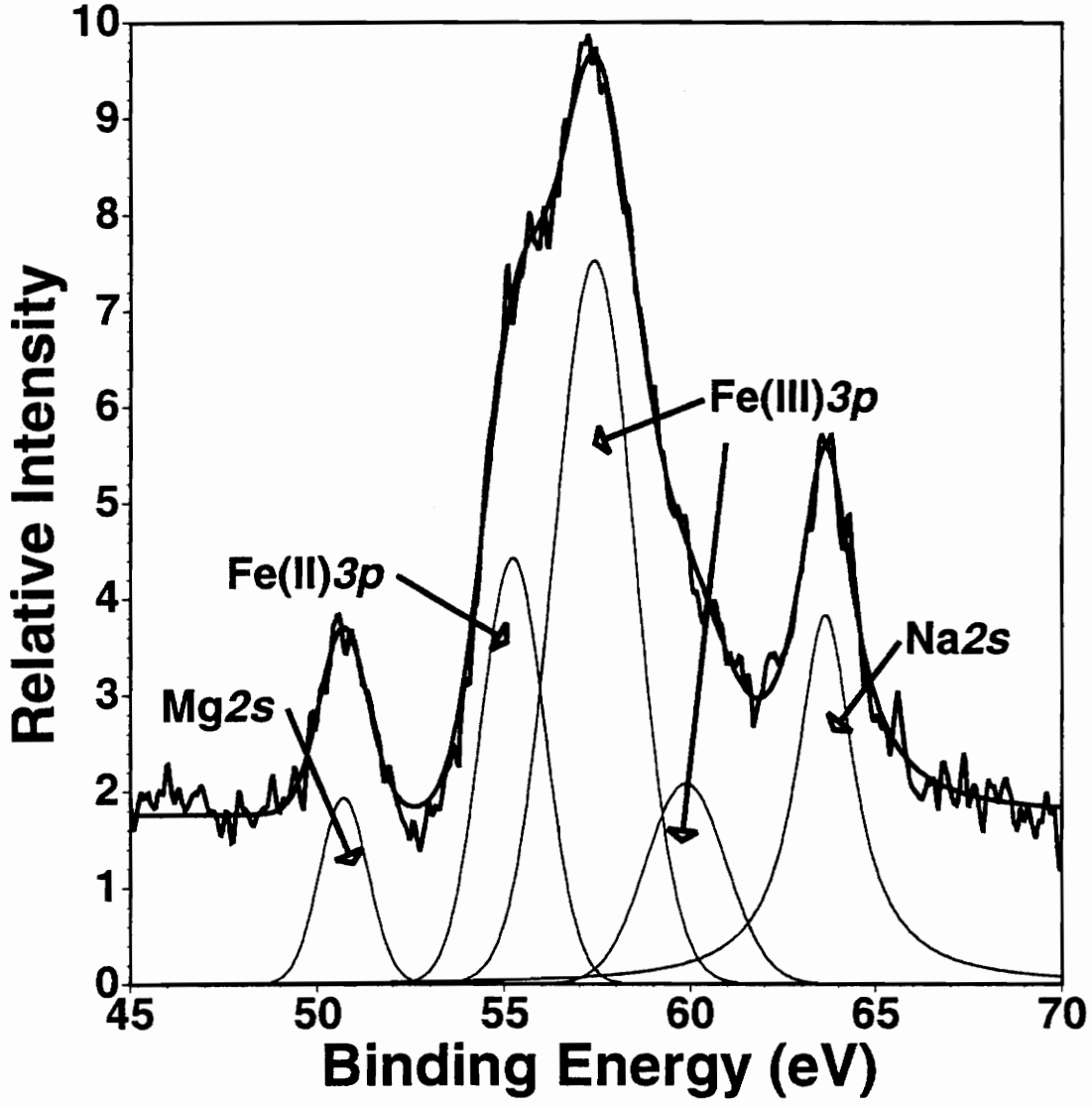

Figure 1. Example of a curve-fit XPS spectra for Na(2s), Fe(3p) and Mg(2s) photolines used in this study. The sum of all curves is seen superimposed on the actual spectra. When determining the Fe(II):Fe(III) ratio, the Fe3p line is fit using the three peaks shown following the example of McIntyre and Zeturak (1977). The relative positions of the three peaks are held constant, as well as their widths and the relative intensities of the two Fe(III) lines. Only the relative intensities of the one Fe(II) line and the two Fe(III) lines are allowed to vary. The Fe(II):Fe(III) ratio is equal to the peak area ratio.

above equation using a value for n determined by microprobe analysis and a value for I which was taken from the XPS data of the untreated sample. Using the calculated σ values and I from the XPS data, the actual values for n were determined for each cation in every sample. Because n for Fe(II) and Fe(III) were determined from the same photoline, their respective σ values were equivalent. The n values for Fe(total), Fe(II), Fe(III), Mg, and Na were then considered proportionately to Si. This cation:Si ratio was needed to compare the XPS data from sample to sample because the sampling volume analyzed in each run varies due to exact sample mounting and instrument conditions. Although I for each photoline varies proportionally to the volume analyzed, the cation:Si ratios for a given sample are independent of the analytic volume allowing ratios to be compared between samples. The changes in cation:Si ratios were then used to follow the near-surface composition of the mineral caused by reaction with the solutions.

In order to test for the development of leached layers on the crocidolite surface within the 30 day length of our experiments, we made use of the Na:Si, Mg:Si, and Fe:Si ratios using the following rationale and approach. The depth from which photoelectrons are derived depends on the attenuation length, λ, of the solid for an electron with the kinetic energy of interest (see Hochella, 1988). There is an exponential reduction in signal as a function of depth which follows the equation:

$$\% \text{ signal} = (1 - e^{-a}) \times 100 \qquad (6)$$

where a is the number of attenuation lengths one wishes to consider. Therefore, 63% of the signal comes from above 1λ, 86% from above 2λ, and 95% from above 3λ (a = 1, 2, and 3, respectively). In practice, the 3λ level in the sample is called the analysis depth. For example, in SiO_2, λ for the Si(2p) photoelectrons ejected by Al Kα X-rays has been measured to be 26Å (Hochella and Carim, 1988), making the 3λ analysis depth 78Å. Because all the photolines for the electrons being analyzed were chosen to have kinetic energies similar to Si(2p), the λ for these cations should be within a few Å of that for Si.

Because the signal attenuates as a function of the electron depth below the surface (Eqn. 6), one can calculate the depth of leaching of one element with respect to another in the near surface (e.g., if the depth of leaching for a given cation with respect to Si is equal to 1λ, one would expect the signal for that cation to be reduced by 63% relative to Si). The above equation can be modified slightly to yield information about the depth of leaching in the following way:

$$\% \text{ signal reduction} = (1 - e^{-x/\lambda}) \times 100 \qquad (7)$$

where x is equal to the depth of cation leaching with respect to some other element. Therefore, knowing the amount of cation signal reduction with respect to another element allows the depth of leaching relevant to that element pair to be determined (e.g., if the Fe signal is reduced by 50% with respect to Si, x = 18Å)(see Fig. 2). We used this scheme to look for the possible leaching of Na, Mg, and Fe relative to Si, and Si relative to Fe in this study.

The approach presented above assumes that the attenuation length is the same in the fresh material and the leached overlayer. This is most likely a very good assumption (Hochella, 1988). However, calculating apparent leaching depths in this way (or any other way) should still only be considered a qualitative measurement. As demonstrated by Hochella (1990), leaching depths are probably not uniform over a surface. Even if leaching depths were uniform, the analyzed surface would have to be flat for the approach presented above to be fully valid. Assuming that surface roughness and uniformity of leaching depth are consistent for all crocidolite samples measured in this study, we can make best use of the calculated leach depths in a relative sense.

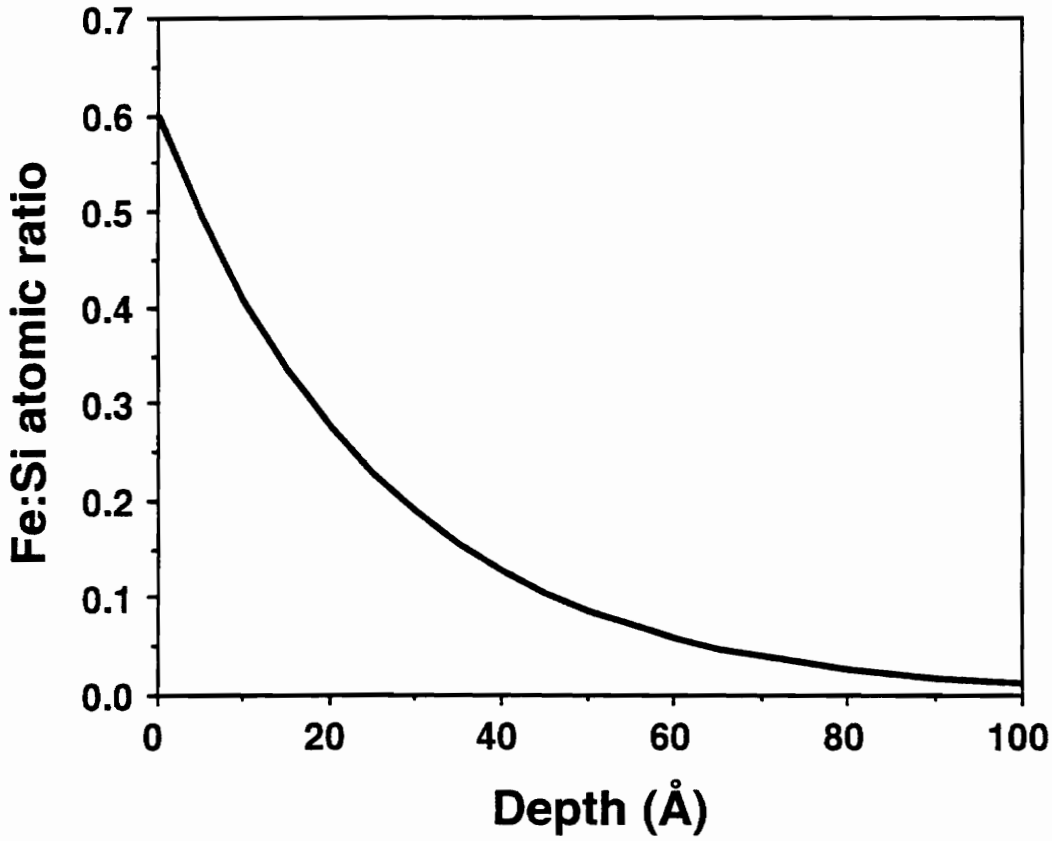

Figure 2. Fe:Si atomic ratio as determined by XPS data vs. hypothetical leaching depth of Fe relative to Si. For example, a Fe:Si atomic ratio of 0.4 as measured by XPS could result by leaching all Fe in the near-surface to a depth of just over 10Å. See text for details.

RESULTS

SEM/AFM Imaging

Figure 3 is an SEM image of randomly dispersed crocidolite fibers that have reacted in solution with citrate for 30 days. The characteristic fluted surface seen on some of the fibers is due to the fact that they are made up of bundles of fibrils (see AFM image in Fig. 4). After 30 days, there is no evidence of a precipitate on the surface of the fibers resolvable with and SEM. The debris seen on the surface is probably smaller crocidolite fibers that are electrostatically attached to the larger fibers.

Solution Analysis

The amount of Fe found in the post-treatment solutions is shown in Figure 5 in terms of nmols of Fe in solution per mg of treated sample. Even after 30 days, there was no detectectable Fe released to solution in the control samples. The introduction of chelators greatly increased the release of Fe from the crocidolite fibers. After 30 days, the amount of Fe released was roughly 200 nmol/mg from the EDTA and desferrioxamine treated fibers and near 100 nmol/mg from the citrate treated fibers.

XPS Analysis

Fe vs. Si surface analysis from crocidolite. The XPS data in Figure 6 shows how the Fe:Si ratios for the control and treated fibers changed over the 30 day period. All the chelator solutions and the control group exhibited an initial rise of the Fe:Si ratio in the first hour and then a decrease of this ratio after 24 hrs. In the control run, this initial action was followed by an increase in the Fe:Si ratio after 30 days. The difference in the Fe:Si ratios between the untreated sample and the average of the 30 day control samples was significant (about 3 standard deviations). The desferrioxamine, EDTA, and citrate treated samples showed slight variations in the Fe:Si ratio relative to

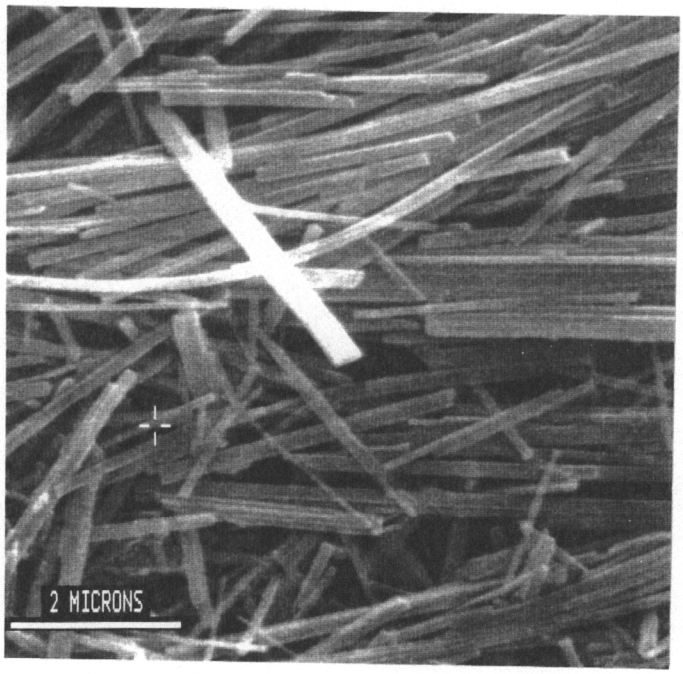

Figure 3. SEM photomicrograph of crocidolite reacted in the presence of citrate for 30 days.

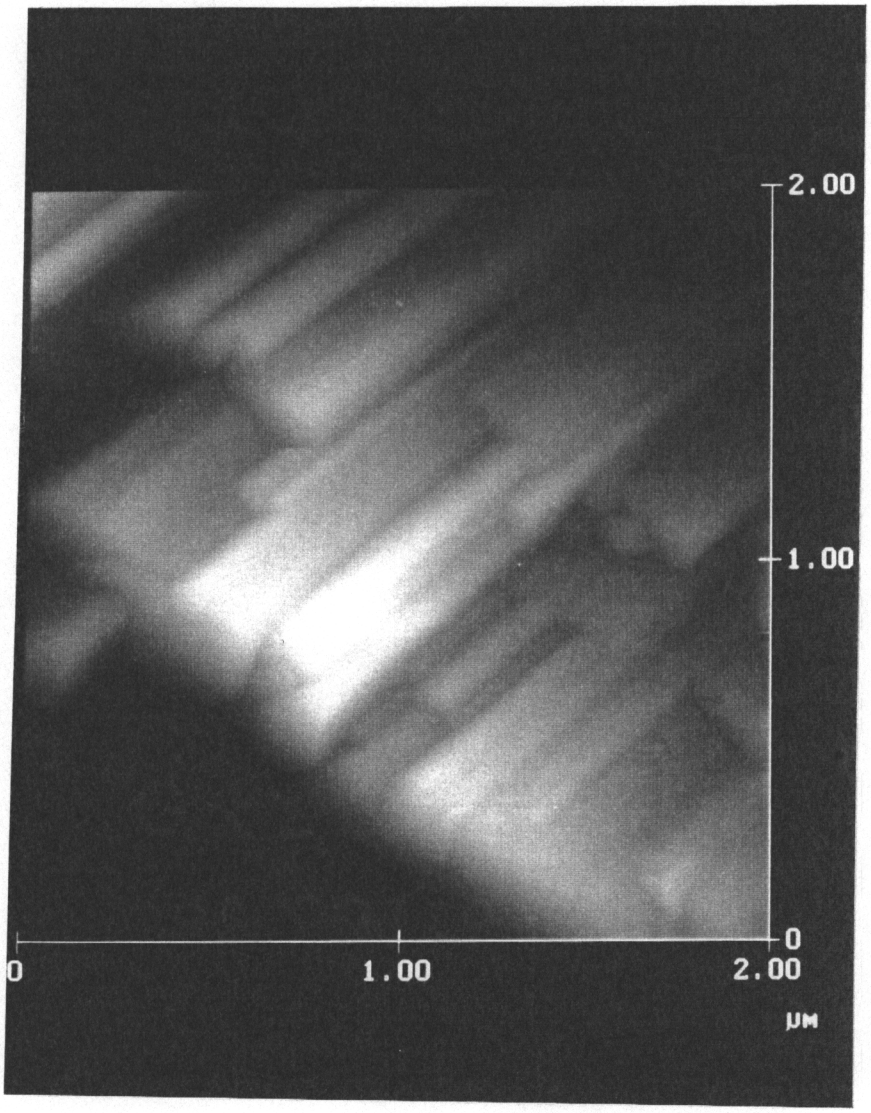

Figure 4. AFM image of the surface of a crocidolite fiber. Individual fibrils that make up each fiber can be easily seen. The fibrils run in the c crystallographic direction. The relief between fibrils in this image is no more than a few hundred Angstroms.

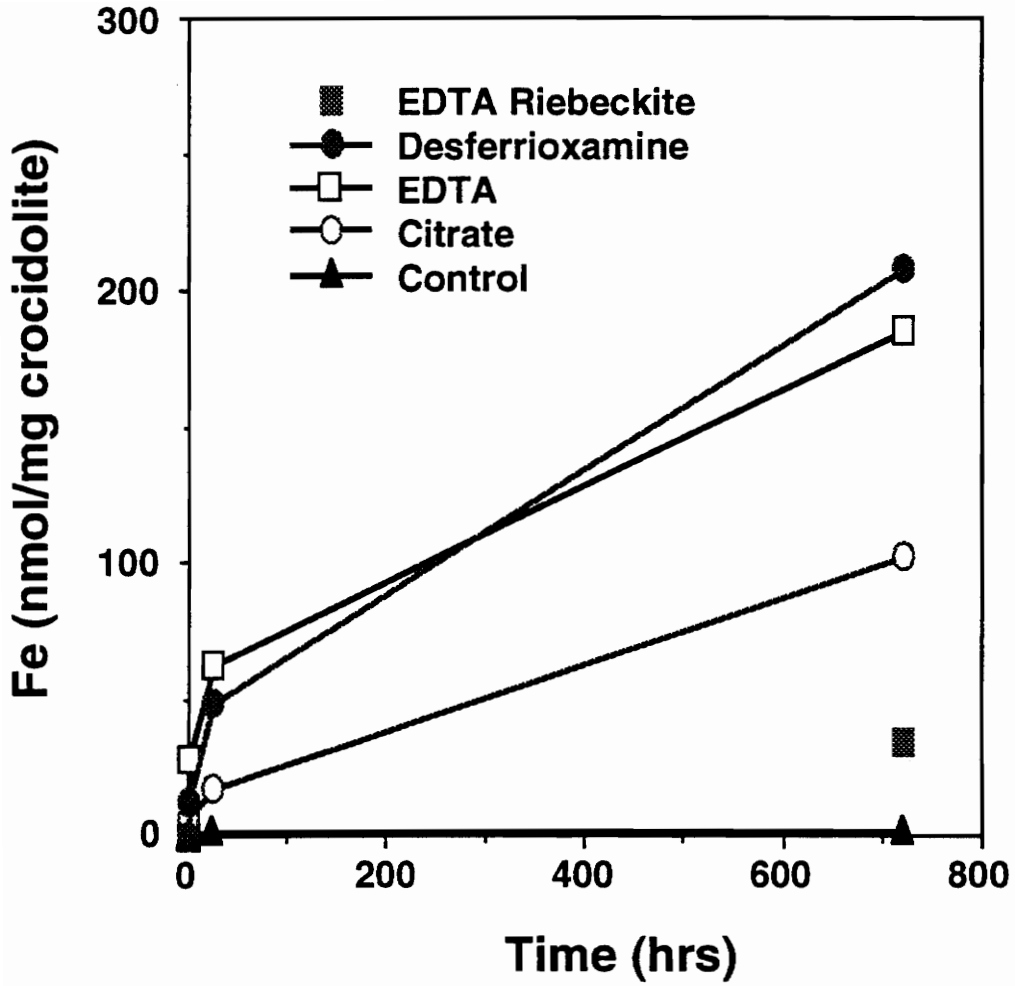

Figure 5. Solution data showing nanomoles of Fe released into the supernatant per milligram of crocidolite or riebeckite. Each point is the average of three identical experiments. Data points are at 1, 24, and 720 hours.

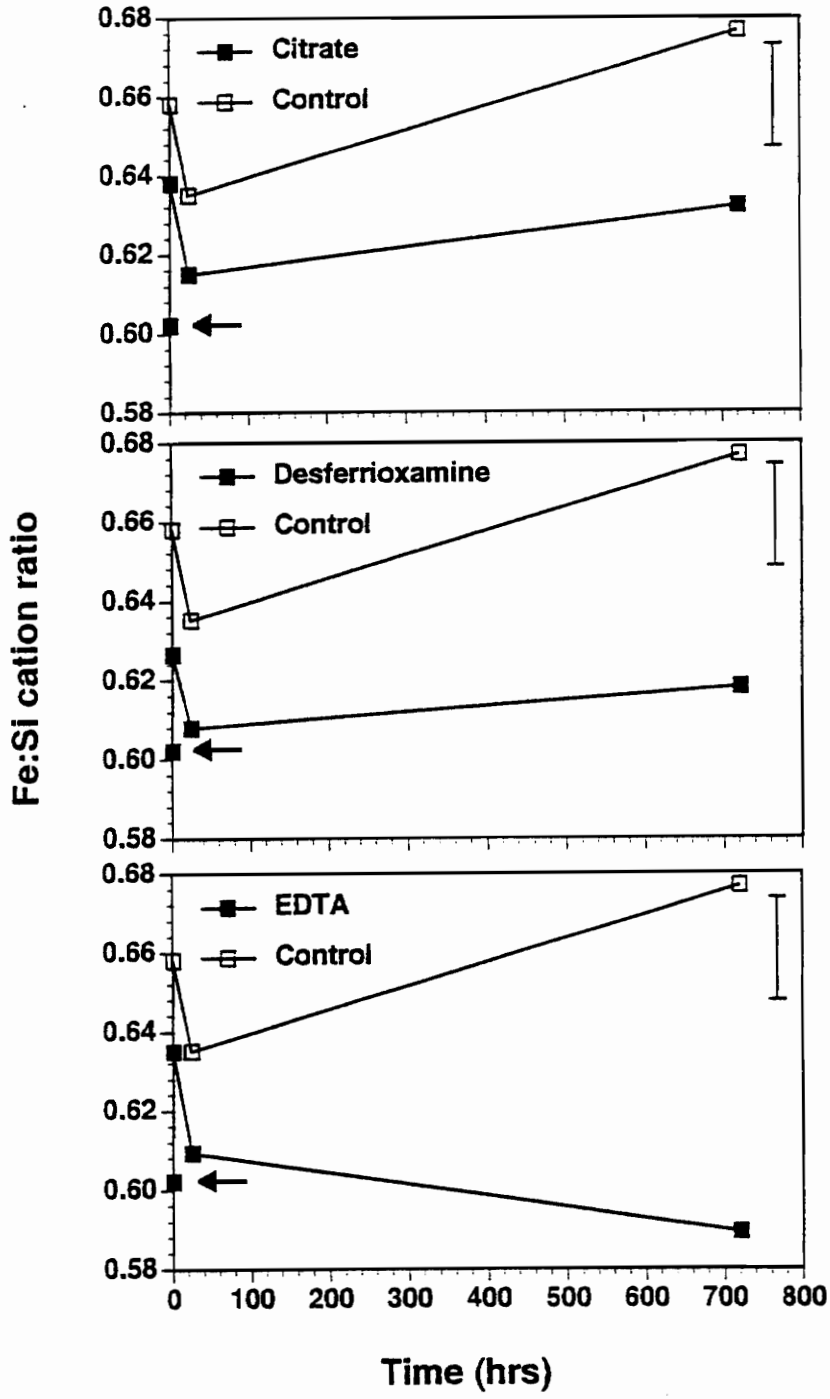

Figure 6. Fe:Si cation ratios as determined by XPS for the control and chelator experiments. Each point is the average of three identical experiments. Data points are at 0, 1, 24, and 720 hours. The bold arrow on the left of each plot represents the starting elemental ratio of the untreated sample. The error bar on the right side of each plot represents one standard deviation as determined from the triplicate runs.

the starting value after reacting in the solutions for 30 days, but these changes were not more than one standard deviation. Therefore, the Fe:Si ratio for the control was significantly higher than those ratios in the chelator groups after 30 days.

Data were also collected to determine how the surface Fe(II):Si and Fe(III):Si ratios changed with time (Fig. 7). The Fe(III):Si ratio in the control increased initially in the first 24 hrs and then remained constant at about 1 standard deviation greater than the untreated sample. The citrate and desferrioxamine treated samples showed a decrease in the ratio of about one standard deviation after 30 days, and the EDTA treated sample less than one standard deviation. Therefore, the Fe(III):Si ratio in the control was greater than that for the chelator groups by 1.5 - 2.5 standard deviations after 30 days.

The Fe(II):Si ratio for the control rose slightly more than one standard deviation after 30 days. The Fe(II):Si ratios also rose in the citrate and desferrioxamine samples by more than two standard deviations while the EDTA samples experienced no change in the ratio after 30 days. All three chelator groups and the control had a statistically similar Fe(II):Si ratio after 30 days (within one standard deviation for desferrioxamine and citrate, less than two standard deviations for EDTA).

Mg and Na vs. Si surface analysis on crocidolite. The Mg:Si ratios are shown in Figure 8. The figure demonstrates that the control had a large decrease (four standard deviations) in the Mg:Si ratio compared to the initial value ratio as did the desferrioxamine and EDTA groups. The citrate group also showed a reduction in the Mg:Si ratio, but less than half as much as the control, desferrioxamine and EDTA groups. The citrate group was the only chelator group with a different Mg:Si ratio than the control after 30 days.

Figure 9 shows the changes in the Na:Si ratios. Only the desferrioxamine group showed a significant decrease in the Na:Si ratios after 30 days (two standard deviations)

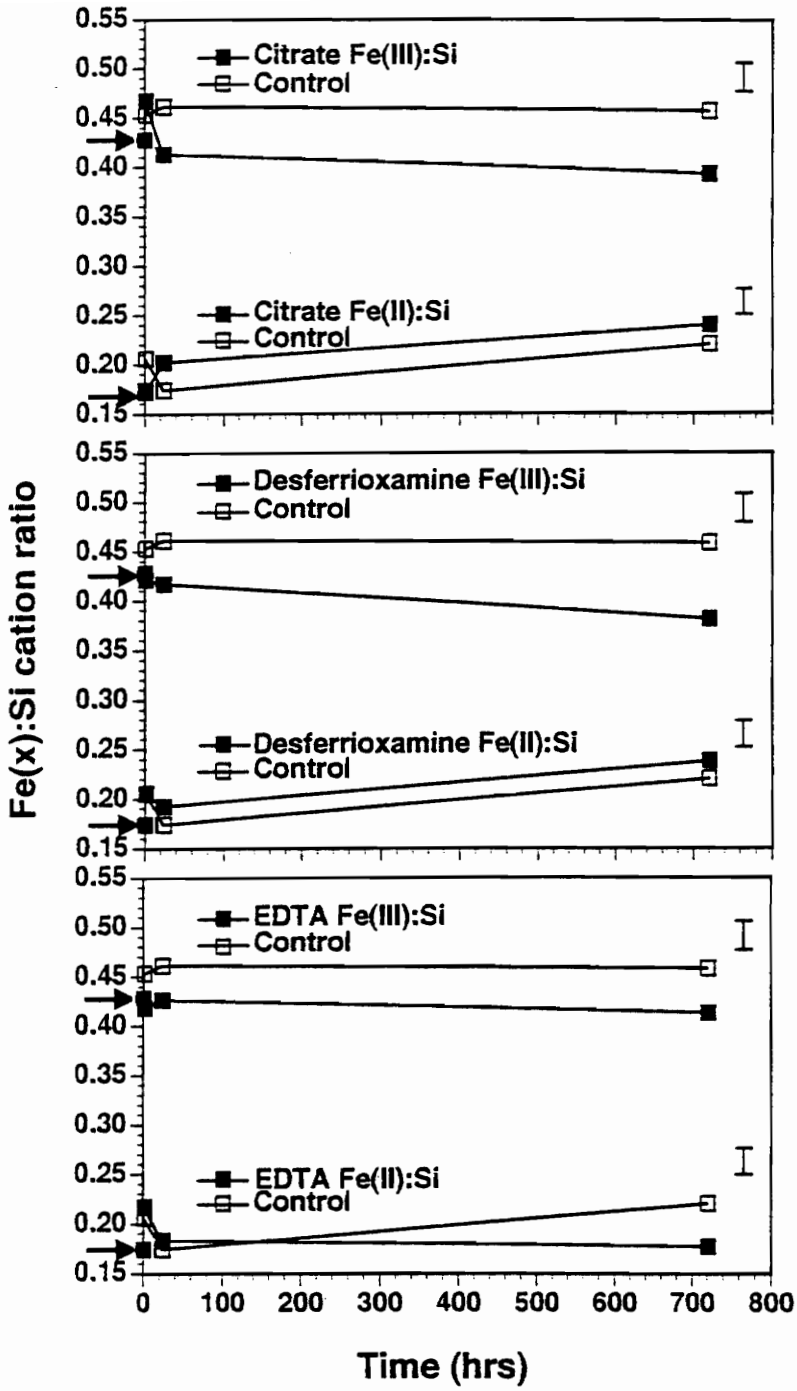

Figure 7. The same as in Fig. 6, except the Fe has been broken down into a ferrous and ferric component.

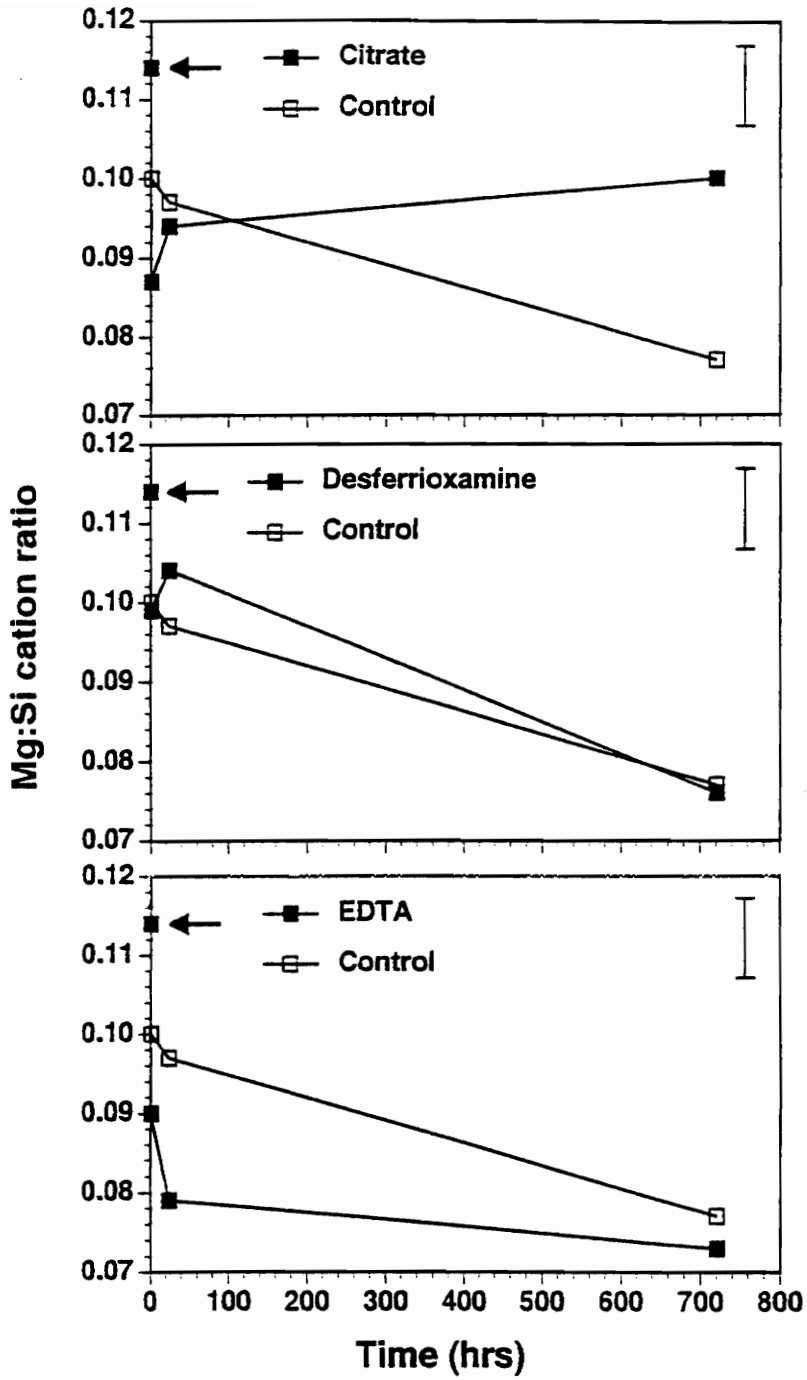

Figure 8. Mg:Si cation ratios vs. experiment duration in exactly the same format as shown in Fig. 6.

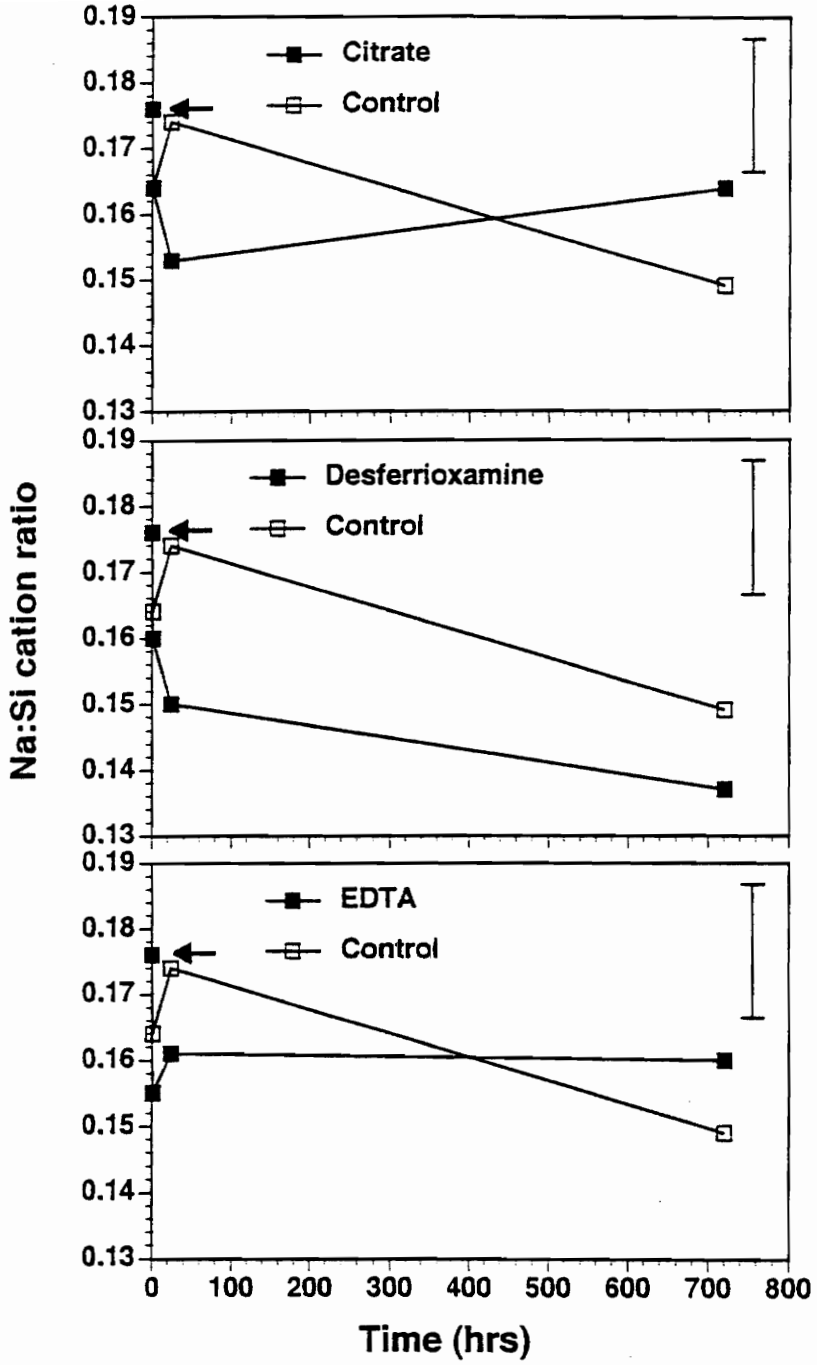

Figure 9. Na:Si cation ratios vs. experiment duration in exactly the same format as shown in Fig. 6.

while the control (just over one standard deviation), citrate and EDTA (less than one standard deviation) groups did not. In the case of all three chelator groups, the Na:Si ratio did not vary more than one standard deviation from the control after 30 days.

DISCUSSION

Control experiments

In the 30 day control runs, the XPS data shows an increase in the Fe:Si ratio. This suggests that a layer exists on the surface that is rich in Fe with respect to Si. Using the leach layer thickness model described in the methods section, the thickness of the Si depleted layer can be calculated at about 5Å. Although the data is consistent with such a depletion layer in which all Si is removed from the top 5Å of the mineral surface, other scenarios are possible. Si could be partially removed from the near-surface, but from deeper in the mineral. Also, it is likely that the leaching depth is quite variable (Hochella, 1990). Nevertheless, the leach layer thickness model gives a relative sense of chemical variations at a surface and makes comparisons with other surfaces easy.

The Si-deficient layer suggested here could be caused by either preferential Si release or precipitation of an Fe-oxide on the surface. Work by White and Yee (1985) on Fe oxidation and reduction in Fe silicates shows that at near neutral pH, the rate of Fe(III) release is greatly decreased due to the initiation of ferric hydroxide or oxyhydroxide precipitation. However, no decrease in the Fe(II):Fe(III) ratio is observed in the XPS results during the 30 day experiment. Therefore, precipitation of Fe(III) is not responsible for the increase in the Fe:Si ratio in the control. Also, although the bulk chemistry data shows that the Fe(II):Fe(III) ratio ≈ 1 in the bulk mineral, the XPS data shows an Fe(II):Fe(III) ratio ≈ 0.4 at the surface. This is most likely from oxidation of the Fe at the surface long before any sample treatment. This surface abundance of nearly

insoluble Fe(III) under these conditions (Baes and Mesmer, 1976) likely hinders Fe release at neutral pH, but allows Si to be preferentially removed.

The XPS data also shows a decrease in the Mg:Si and Na:Si ratios at 30 days that is equivalent to a 5 Å Na and a 10 Å Mg depleted layer with respect to Si. Because we have shown that Si was released from the surface, Na and Mg must have been leached as well, but to a slightly greater depth.

Due to the nature of a crocidolite fiber bundle, surface chemistry internal to the bundles (i.e., on the surfaces of fibrils accessible to solutions along grain boundaries) is probably an important component of the cell-mineral reaction. These surfaces would not be observable to classic surface-sensitive spectroscopies, but would certainly contribute to changes in the solution chemistry, and reactions at these surfaces can be studied directly with high resolution transmission electron microscopy (HRTEM). Groups that have looked at dissolution reactions and weathering processes internal to mineral grains with HRTEM include Ahn and Peacor (1987), Banfield and Eggleton (1988, 1990), and Banfield et al. (1991). Specifically for crocidolite fibers, inter-fibril regions are likely to contain sheet silicates (perhaps biotite) according to the HRTEM results of Ahn and Buseck (1991, and references therein). The sheet silicates would be only minor to trace mineral components in a bulk sense, but they could have moderate or conceivably greater influence in reactions with solutions.

Chelator experiments

The release of Fe in the chelator solutions can be broken down into its Fe(II) and Fe(III) components using XPS data. As noted in the results section, the Fe(II):Si and Fe(III):Si ratios for the 30 day EDTA, desferrioxamine, and citrate groups do not vary considerably from the untreated sample, but trends in the Fe(II):Si and Fe(III):Si ratios appear as though they will converge with time for at least desferrioxamine and citrate.

This is probably the result of the beginnings of the removal of the oxidized layer at the surface mentioned in the previous section. As the outer oxidized layer dissolves away, the surface properties become more like those of the bulk, where Fe(II):Fe(III) ≈ 1, causing the Fe(II):Si and Fe(III):Si ratios to move towards convergence.

After 30 days in the presence of the solutions with chelators, the total Fe:Si ratios do not significantly change. From this, one might infer that the crocidolite fibers are dissolving congruently, that is Si is being released at a rate in stoichiometric proportion to Fe according to the composition of the mineral. One only need to assume that the disappearance of the fiber is a function of the release of Fe or Si, and one could easily calculate a fiber lifetime. But it has been shown or inferred in other studies (e.g., Berner et al., 1985; Mogk and Locke, 1988; Hochella et al., 1988; Hellmann et al., 1990) that release data to solution and XPS observations generally do not have a simple correlation. This is because the solution and XPS data are measuring two different things. The release-to-solution data gives the total number of cations which have been liberated from the solid and have not participated in any kind of reprecipitation reaction. This data says nothing about from where the cations have come. On the other hand, XPS data gives the composition of the top several 10's of Angstroms over a large area of the sample. XPS cannot "see" what is happening on internal surfaces, and XPS data does not give the distribution of cations within the depth of analysis (unless you do angle-resolved XPS, but this is not possible on rough surfaces or fibers). Finally, the data cannot be used to determine leaching depth heterogeneity. Taken together, this means that release-to-solution data cannot be used to predict XPS results, and visa versa. This issue was specifically tested in a study of crocidolite dissolution by Gronow (1987) and shown to be true. In fact, in this study, Gronow showed crocidolite dissolution to be incongruent after 1024 hours between pH's of 4 and 9, yet XPS showed no change in the average surface chemistry at least over the first 50 hours of reaction at pH 4. Our group has also

shown the lack of simple correlation between solution release data and XPS observations in a study of the dissolution of albite (Hellmann et al., 1990). Therefore, we cannot say with any confidence that Si is released in stoichiometric proportion to Fe even though the XPS data shows that the Fe:Si ratio does not change from the untreated to the 30 day treated sample. However, if we restrict our discussion just to Fe release, we can estimate the Fe-release lifetime of a fiber as shown below.

Fe:Si fluctuations in the first 24 hours

The Fe:Si ratios determined from the XPS data for all the data groups show an increase in the first hour followed by a decrease in the following hours up to the 24 hour point. The reason for this consistent fluctuation is not known, but presumably it has something to do with highly reactive sites on the untreated fiber surface. The chelators probably do not play a role in this fluctuation because the same behavior is seen in the control group. We assume here that this fluctuation is not important in determining the long term effects that molecular chelators have on crocidolite dissolution.

Fe release lifetime in chelator solutions

The rate of Fe release from the mineral was calculated from the change in Fe concentration between 1 and 30 days. Because of the initial perturbation in the dissolution rate discussed above, the amount of Fe released into solution in the first day is not a good estimate of long term Fe release. To obtain a more reasonable Fe release rate, a rate constant, k, was determined using the concentration change between the day 1 and day 30 data points for the control and each chelator group. The use of one day as an appropriate starting point is justified by the crocidolite dissolution study of Gronow (1987) who showed that dissolution had reached a steady state after this period of time.

The model from Hume and Rimstidt (1992) was used to estimate the Fe release lifetime of crocidolite fibers as follows:

$$t = (3/4)(d/V_m k) \quad (8)$$

where t is the lifetime, d is the diameter of the fiber, and V_m is the molar volume divided by the number of Fe atoms in the stoichiometric formula. Table 1 shows the values for *k* and the Fe release lifetimes for 0.25 μm fibers (the mean diameter of fibers used in this study) and 1.0 μm diameter fibers. If the rate constants were calculated from longer term experiments, it is likely that they would be smaller. As a result, the predicted Fe release lifetime would be even longer.

Our estimate of Fe release lifetimes of crocidolite fibers should be used with caution. In the lung, fibers are not necessarily in a free fluid. They may be engulfed in scavenging cells (phagocytes) and subjected to relatively extreme chemistries (particularly lower pH's) compared to typical fluids in the lung. This would almost certainly result in shorter lifetimes, as would increasing the ambient temperature (the body is at 37°C, approximately 14°C higher than our experiments). Further, Lund and Aust (1990) showed that the presence of ascorbate, which is found in physiological fluids, can increase the release rate of Fe(II) from crocidolite in the first 36 hours under similar conditions to the control and chelator experiments of this study. On the other hand, fibers in lungs are also commonly partially covered with iron-rich coatings believed to be derived from proteins such as hemosiderin and ferritin. This could significantly slow the rate of Fe release from the fiber. Finally, many other agents in lung fluids which have not been tested may have major effects on fiber chemistry and dissolution.

The Fe release lifetimes for crocidolite fibers of many decades to hundreds of years correspond well to what is already known about the biodurability of asbestos minerals from epidemiological, *in vivo*, and lung burden studies. Some time ago, Wagner et al. (1974) noted that rats continuously exposed to amphibole fibers suffered a ever

Table 1. Estimates of iron release lifetimes of crocidolite at pH 7.5.

	k (mol croc/m^2s)	Lifetime (yrs) for d=0.25 μm	Lifetime (yrs) for d=1.0 μm
Control	≈ 0	–	–
Citrate	1.03×10^{-12}	106	422
Desferrioxamine	7.15×10^{-13}	151	606
EDTA	1.34 x 10-12	81	324

increasing lung burden, while rats continuously exposed to chrysotile fibers showed only a moderate lung burden which leveled off with time. Jones et al. (1989) more recently came to the same conclusion. This fiber accumulation pattern in lung tissue has also been shown to be the same in humans (Churg, 1993, and references therein). This is all consistent with Hume and Rimstidt (1992) who studied the dissolution behavior of chrysotile fibers at a temperature and pH range consistent with human lung conditions. For these conditions, they estimated that a 1 μm diameter fiber of chrysotile will completely dissolve in less than one year. Therefore, it is no surprise that the crocidolite burden recovered from autopsied human lungs is always considerably greater than the proportion of crocidolite fiber dust in the air source responsible for the lung contamination (e.g., Wagner et al., 1982; Gardner et al., 1986; Churg, 1988). Either chrysotile fibers are not making it into the lung through the upper bronchial tubes relative to the crocidolite fibers for mechanical/aerodynamic reasons, or crocidolite fibers are much more biodurable. A number of studies have shown that the former hypothesis is not true (Roggli and Brody, 1984; Churg et al., 1984; Roggli et al., 1987; Coin et al., 1992), leaving the later as the most probable cause. Finally, as already mentioned above, it is now clear from epidemiological studies that crocidolite fibers are much more pathogenic than chrysotile fibers in man. From this, one can reasonably assume that fiber durability is at least indirectly related to the generation of lung disease. It follows that fiberglass, which shows only poor durability in lung tissue as would be expected for an amorphous silicate, should have little if any pathogenic potential. Indeed, this has been shown to be the case (McDonald, 1990).

Implications for mineral-induced pathogenesis

The observations of crocidolite dissolution in the presence of chelators *in vitro* should be relevant to biological applications. Because the solutions used in this study

were meant to model conditions in the human lung, we can begin to hypothesize how inhaled crocidolite changes in the lung and what effect these changes may have on human health.

We have determined, as first shown by Aust and Lund (1990), that when chelators are introduced into a solution with crocidolite fibers, the rate of Fe release increases dramatically. One of the chelators from this study, citrate, is found in physiological fluids in humans. Therefore, crocidolite dissolution would provide a considerable and long-lasting source of Fe to promote DNA damage as long as the fiber remained present in the lung. The estimates for fiber lifetime from this study shows that where citrate is present, the average crocidolite fiber will persist much longer than a human life span.

Even if one involves processes in the lung that could significantly increase the dissolution rate of the fibers (several are mentioned above), the Fe release lifetimes would still be tens to hundreds of times longer than chrysotile. Therefore, our conclusions are still consistent with fiber lung burdens found in autopsied lungs.

Future models for mineral-induced pathogenesis will most likely include reactions at the mineral-physiological fluid interface. This study is one of the first in a long series that will be needed to meet this objective.

REFERENCES

Ahn, J.H. and Buseck, P.R. (1991) Microstructures and fiber-formation mechanisms of crocidolite asbestos. American Mineralogist, 76, 1467-1478.

Ahn, J.H. and Peacor, D.R. (1987) Kaolinitization of biotite: TEM data and implications for an alteration mechanism. American Mineralogist, 72, 353-356.

Aust, A.E. and Lund, L.G. (1990) The role of iron in asbestos-catalyzed damage to lipids and DNA. Biological Oxidation Sytems, 2, 597-605.

Aust, A.E. and Lund, L.G. (1991) Iron mobilization from crocidolite results in enhanced iron-catalyzed oxygen consumption and hydroxyl radical generation in the presence of cysteine. In: Mechanisms in Fibre Carcinogenesis, Brown, R.C., Hoskins, J.A., and Johnson, N.F., eds., NATO ASI Series, Plenum Press, New York, 397-405.

Baes, C.F., Jr. and Mesmer, R.E. (1976) The Hydrolysis of Cations., John Wiley & Sons, New York, 489 pp.

Banfield, J.F. and Eggleton, R.A. (1988) Transmission electron microscope study of biotite weathering. Clays and Clay Minerals, 36, 47-60.

Banfield, J.F. and Eggleton, R.A. (1990) Analytical transmission electron microscope studies of plagioclase, muscovite, and K-feldspar weathering. Clays and Clay Minerals, 38, 77-89.

Banfield, J.F., Jones, B., F. and Veblen, D.R. (1991) An AEM-TEM study of weathering and diagenesis, Abert Lake, Oregon: I. Weathering reactions in the volcanics. Geochimica et Cosmochimica Acta, 55, 2781-2793.

Barrett, J.C., Lamb, P.W. and Wiseman, R.W. (1989) Multiple mechanisms for the carcinogenic effects of asbestos and other mineral fibers. Environmental Health Perspectives, 81, 81-89.

Berner, R.A., Holdren, G.R., Jr. and Schott, J. (1985) Surface layers on dissolving silicates. Geochimica et Cosmochimica Acta, 43, 1173-1186.

Brown, R.C., Carthew, P., Hoskins, J.A., Sara, E. and Simpson, C.F. (1990) Surface modification can affect the carcinogenicity of asbestos. Carcinogenesis, 11, 1883-1885.

Campbell, W.J., Huggins, C.W. and Wylie, A.G. (1980) Chemical and physical characterization of amosite, chrysotile, crocidolite, and nonfibrous tremolite for oral ingestion studies by the National Institute of Environmental Health Sciences.

Chao, C. and Aust, A.E. (1992) Photochemical reduction of ferric iron by chelators results in DNA strand breaks. Archives of Biochemistry and Biophysics, 300, 544-550.

Churg, A. (1988) Chrysotile, tremolite, and mesothelioma in man. Chest, 93, 621.

Churg, A. (1993) Asbestos lung burden and disease patterns in man. In: Health Effects of Mineral Dusts, Guthrie, G.D., Jr. and Mossman, B.T., eds., Reviews in Mineralogy, 28, Mineralogical Society of America, Washington D.C., 410-426.

Churg, A., DePaoli, L., Kempe, B. and Stevens, B. (1984) Lung asbestos content in chrysotile workers with mesothelioma. American Reviews on Respiratory Disease, 130, 1042-1045.

Coin, P.G., Roggli, V.L. and Brody, A.R. (1992) Deposition, clearance, and translocation of chrysotile asbestos from peripheral and central regions of the lung. Environmental Research, 58, 97-116.

Craighead, J.E., Abraham, J.L., Churg, A., Green, F.H.Y., Kleinerman, J., Pratt, P.C., Seemayer, T.A., Vallaythan, V. and Weill, H. (1982) The pathology of asbestos-

associated diseases of the lungs and pleural cavities: Diagnostic criteria and proposed grading scema. Archives of Pathology and Laboratory Medicine, 106, 544-596.

Gardner, M.J., Winter, P.E., Pannett, B. and Powell, C.A. (1986) Follow up study of workers manufacturing chrysotile asbestos cement products. British Journal of Industrial Medicine, 43, 726.

Goodlick, L.A. and Kane, A.B. (1986) Role of reactive oxygen metabolites in crocidolite asbestos toxicity to mouse macrophages. Cancer Research, 46, 5558-5566.

Gronow, J.G. (1987) The dissolution of asbestos fibers in water. Clay Minerals, 22, 21-35.

Gupta, R.P. and Sen, S.K. (1974) Calculation of multiplet structure of core *p*-vacancy levels. Physical Review B, 10, 71-77.

Guthrie, G.D., Jr. and Mossman, B.T. (1993) Merging the geological and biological sciences: An intergrated approach to the study of mineral-induced pulmonary diseases. In: Health Effects of Mineral Dusts, Guthrie, G.D., Jr. and Mossman, B.T., eds., Reviews in Mineralogy, 28, Mineralogical Society of America, Washington D.C., 1-5.

Hellmann, R., Eggleston, C.M., Hochella, M.F., Jr. and Crerar, D.A. (1990) The formation of leached layers on albite surfaces during dissolution under hydrothermal conditions. Geochimica et Cosmochimica Acta, 54, 1267-1281.

Hochella, M.F., Jr. (1988a) Auger electron and X-ray photoelectron spectroscopies. In: Spectroscopic Methods in Mineralogy and Geology, Hawthorne, F.C., eds., Reviews in Mineralogy, 18, Mineralogical Society of America, Washington D.C., 573-638.

Hochella, M.F., Jr. (1990) Atomic structure, microtopography, composition, and reactivity of mineral surfaces. In: Mineral-Water Interface Geochemistry,

Hochella, M.F., Jr. and White, A.W., eds., Reviews in Mineralogy, 23, Mineralogical Society of America, Washington, D.C., 87-132.

Hochella, M.F., Jr. (1993) Surface chemistry, structure, and reactivity of hazardous mineral dust. In: Health Effects of Mineral Dusts, Guthrie, G.D., Jr. and Mossman, B.T., eds., Reviews in Mineralogy, 28, Mineralogical Society of America, Washington D.C., 275-308.

Hochella, M.F., Jr and Carim, A.H. (1988b) A reassessment of electron escape depths in silicon and thermally grown silicon dioxide thin films. Surface Science, 197, L260-L268.

Hume, L.A. and Rimstidt, J.D. (1992) The biodurability of chrysotile asbestos. American Mineralogist, 77, 1125-1128.

Jones, A.D., Vincent, J.H., McIntosh, C., McMillan, C.H. and Addison, J. (1989) The effect of fiber durability on the hazard potential of inhaled chrysotile asbestos fibers. Experimental Pathology, 37, 98-102.

Klockars, M., Hedenborg, M. and Vanhala, E. (1990) Effect of two particle surface-modifying agents, polyvinylpyridine-N-oxide and carbomethylcellulose, on the quartz and asbestos mineral fiber-induced production of reactive oxygen metabolites by human polymorphonuclear leukocytes. Archives of Environmental Health, 45, 8-14.

Lund, L.G. and Aust, A.E. (1990) Iron mobilization from asbestos by chelators and ascorbic acid. Archives of Biochemistry and Biophysics, 278, 60-64.

Lund, L.G. and Aust, A.E. (1992) Iron mobilization from crocidolite asbestos greatly enhances crocidolite-dependent formation of DNA single-strand breaks in øX174 RFI DNA Carcinogenesis, 13, 637-642.

McDonald, J.C. (1990) Cancer risks due to asbestos and man-made fibres. Recent Results in Cancer Research, 120, 122-133.

McDonald, J.C. and McDonald, A.D. (1986a) Epidemiology of malignant mesothelioma. In: Asbestos Related Malignancy, Antman, K. and Aisner, J., eds., Grune and Stratton, New York, 57-79.

McDonald, J.C. and McDonald, A.D. (1986b) Epidemiology of asbestos-related lung cancer. In: Asbestos-Related Malignancy, Antman, K. and Aisner, J., eds., Grune and Stratton, New York, 31-56.

McIntyre, N.S. and Zetaruk, D.G. (1977) X-ray photoelectron spectroscopic studies of iron oxides. Analytical Chemistry, 49, 1521-1529.

Mogk, D.W. and Locke, W.W., III (1988) Application of auger electron spectroscopy (AES) to naturally weathered hornblende. Geochimica et Cosmochimica Acta, 52, 2537-2542.

Nolan, R.P. and Langer, A.M. (1993) Limitations of the Stanton Hyposthesis. In: Health Effects of Mineral Dusts, Guthrie, G.D., Jr. and Mossman, B.T., eds., Reviews in Mineralogy, 28, Mineralogical Society of America, Washington D.C., 308-326.

Roggli, V.L. and Brody, A.R. (1984) Changes in numbers and dimensions of chrysotile asbestos fibers in lungs of rats following short-term exposure. Experimental Lung Research, 7, 133-147.

Roggli, V.L., George, M.H. and Brody, A.R. (1987) Clearance and dimensional changes of crocidolite asbestos isolated from lungs of rats following short-term exposure. Environmental Research, 42, 94-105.

Stanton, M.F., Layard, M., Tegeris, A., Miller, E., May, M., Morgan, E. and Smith, A. (1981) Relation of particle dimension to carcinogenicity of amphibole asbestoses and other fibrous minerals. Journal of the National Cancer Institute, 67, 965-975.

Vu, V.T. (1993) Regulatory approaches to reduce human health risks associated with exposures to mineral fibers. In: Health Effects of Mineral Dusts, Guthrie, G.D.,

Jr. and Mossman, B.T., eds., Reviews in Mineralogy, 28, Mineralogical Society of America, Washington D.C., 545-554.

Wagner, J.C. (1991) The discovery of the association between blue asbestos and mesotheliomas and the aftermath. British Journal of Industrial Medicine, 48, 399-403.

Wagner, J.C., Berry, G. and Pooley, F.D. (1982) Mesotheliomas and asbestos type in asbestos textile workers: A study of lung contents. British Medical Journal, 285, 603.

Wagner, J.C., Berry, G., Skidmore, J.W. and Timbrell, V. (1974) The effects of the inhalation of asbestos in rats. British Journal of Cancer, 29, 252-269.

Wagner, J.C., Sleggs, C.A. and Marchand, P. (1960) Diffuse pleural mesotheliomas and asbestos exposure in the north western Cape Province. British Journal of Industrial Medicine, 17, 260-271.

White, A.F. and Yee, A. (1985) Aqueous oxidation-reduction kinetics associated with coupled electron-cation transfer from iron-containing silicates at 25°C. Geochimica et Cosmochimica Acta, 49, 1263-1275.

VITA

Andrew J. Werner was born September 11, 1970 in Arlington, Virginia. He spent the majority of his childhood and adolescence years in Northern Virginia, although he spent his last year before college in Charlottesville, Virginia. His initial ambitions, to become an engineer like his father, attracted him to VIP & SU, but he quickly learned that his interests were aimed more at becoming a scientist. He went on to study in the Geology department at VPI & SU. Mineralogy intrigued Andrew when he first began to study geology and later became his main learning interest. He received his Bachelor of Science in Geology at VPI & SU in Spring 1992. After this, he continued his education at VPI & SU in the Masters program. Andrew found a new interest in mineral surface geochemistry because some of this discipline's research was in the forefront of science. He studied for two more years to receive a Master of Science in Geology in the area of mineral surface geochemistry.